

SUPPLEMENTARY MATERIALS

Materials and Methods

TGT synthesis.

TGTs were used with rupture forces of 12pN, 33pN, and 54pN, and were chosen based on a previous report, which showed an integrin tear off threshold at 40 pN¹. Integrin-binding TGTs were generated, by conjugating cyclic peptide RGDfK to one DNA strand of a rupturable dsDNA tether. The other strand of the dsDNA was labeled with an acrydite tag at a desired position, for tethering to the hydrogel (Fig. 1C). The position of the RGDfK on the dsDNA determines tension at which the tethers rupture. The complementary ssDNA was acrydite-labeled 5-Acrydite/GGC CCG CAG CGA CCA CCC-3. The ssDNAs were purchased from Integrated DNA technologies, Inc. The tension tolerance is determined by the position of the reactive ThioMC3 and fluorescent Cy3 label in the nucleic acid sequence. The ThioMC3 positions in different TGTs with the indicated tension tolerance are given below:

54 pN TGT: 5-/5ThioMC3-D/ GGG TGG TCG CTG CGG GCC /Cy3/-3

33 pN TGT: 5-/5Cy3/GGGTGGTCGCT/iThioMC6-D/GCGGGCC/-3

12 pN TGT: 5-/5Cy3/GGGTGGTCGCTGCGGGCC/3ThioMC3-D/-3

The cyclic peptide RGDfK-NH₂ (catalog #: PCI-3696-PI) from Peptides International, Inc. RGDfK was conjugated to ThioMC3 on ssDNA using the hetero-bifunctional crosslinker Sulfo-SMCC (22622, Thermo Fisher Scientific Inc.), which has reactive maleimide and NHS ester groups on the two ends. The maleimide reacted with the thiol-modified DNA and the NHS covalently coupled to the N-terminal amine on RGDfK. The RGDfK-DNA and acrydite-DNA were then annealed in 'annealing buffer' (150mM NaCl, 10mM Tris, PH 7.4) at room temperature. In Phosphate Buffered Saline (PBS) at pH 7.4, the melting temperature of the dsDNA tethers is 73 °C.

The control, non-rupturable tether was prepared by reacting an Acrylate PEG-NHS ester (3500 MW PEG; JenKem Technology USA, Allen, TX) with RGDfK-NH₂ at a molar ratio of 24:1 (PEG-NHS: RGD-NH₂), at room temperature in PBS at pH 8.0. Unreacted PEG-NHS was removed, using a 10K MW Pierce Concentrator PES (Thermo Scientific, Waltham, MA).

Hydrogel preparation and characterization.

To generate hydrogels with different Young's moduli, 7.5kDa PEG diacrylate macromers (Jenkem Technology) were mixed at 7 and 10 wt% in PBS, containing the TGT and 0.1% (w/v) lithium phenyl-2,4,6-trimethylbenzoylphosphinate (LAP) as a photoinitiator². The double ring structure of Cy3 sterically hinders the reactivity of methacrylamide groups in the 54 pN probes, during photo polymerization with PEG-diacrylate. Therefore, the initial tether concentration was adjusted in the prepolymer solution to achieve 1.5 μM of covalently bonded RGD for all samples. The initial TGT

concentrations were 1.5 μM (54pN), 1.5 μM (33pN) and 2.2 μM (12pN). The prepolymer solution was then pipetted into 1 mm thick, circular Teflon molds of 5 mm diameter, and exposed to 10 mW/cm^2 UV light (365 nm) for 90s at room temperature. The hydrogel disks were then detached from the mold.

Mechanical analyses of the resulting hydrogels were performed on water swollen hydrogel disks, at room temperature with an MTS Insight mechanical testing apparatus at a strain rate of 20%/min. The compressive modulus was determined from the linear region corresponding to 0-5% strain. The relative tether concentrations bound to the hydrogels were determined from Cy3 fluorescence measurements. The fluorescence intensity was quantified before and after washing, and different preparations were compared to assess the relative amounts of covalently bound TGTs on each of the hydrogels (Fig. S1). Imaging was performed using a Zeiss LSM 710 NLO laser scanning confocal microscope (Carl Zeiss, Thornwood, NY, USA).

Cell culture conditions, cell density determination, and area analyses.

B16F1, U87MG cell lines (from ATCC) were cultured in DMEM supplemented with 10% FBS and penicillin/streptomycin (100 U/ml and 100 mg/ml), at 37 °C in a 5% CO_2 environment, while CHOK1 (ATCC) cells were cultured in Alpha-MEM under the same conditions. Cells were passaged upon reaching confluence, and were detached with 3mM EDTA, in order to minimize integrin degradation during cell harvesting.

Cells were seeded on gels with elastic moduli of 13 and 22 kPa that were surface modified with RGD-functionalized TGTs with tension tolerances of 12, 33, or 54 pN. Cell were detached from culture dishes with 3mM EDTA, to preserve integrins. Cell seeding densities were controlled by suspending 2.8×10^6 cells/mL in Dulbecco's Modified Eagle Medium (DMEM) supplemented with 0.5% Fetal Bovine Serum (FBS) and penicillin/streptomycin (100 U/ml and 100 mg/ml), and then 30 μl of the cell suspension (8.4×10^4 cells/disk) was applied to the substrates for 30 minutes at 37 °C under 5% CO_2 . The non-rupturable PEG-RGD was used as a control.

Cell viability was assessed with a Live/Dead assay (Invitrogen), based on Calcein staining, and laser scanning confocal microscopy (5x, Zeiss LSM710). Prior to imaging, gels were incubated in PBS containing 4 mM Calcein AM ($\lambda_{\text{em}} = 515$ nm, Invitrogen) for 30 minutes, in order to stain viable cells. This was followed washing the cells 3x with PBS.

The number of bound cells per area, on each substrate, was determined by manually counting the number of Calcein positive cells within a defined imaging area, using the Image J cell count plug-in (<http://rsb.info.nih.gov/ij/>). In order to estimate the average number of cells per square millimeter, we counted the number of cells in the field of view of at least two images, at a magnification of 5x. This imaged ~20% of the total surface of the gel. Prior findings indicated that analysing greater than 10% of the total surface area constitutes a statistically significant sampling of the entire surface.³

The spread cell area was assessed from DIC images at a magnification of 20x, and use of ImageJ (<http://rsb.info.nih.gov/ij/>). The image threshold was manually set to 95% of the pixel intensity. The cells were selected with the Wand Function, and the area was calculated using the built-in area calculator plug-in under the measurement tab in ImageJ.

Immunofluorescence imaging of vinculin staining and analysis.

For vinculin immunofluorescence imaging, cells were seeded at a density of 10^6 cells/mL of which 30 μ l were added per gel (10^4 cells/gel). The lower seeding density used facilitated the analysis, but did not affect the results, which reported the fraction of vinculin positive cells rather than the absolute number per area.

Vinculin staining was visualized from immunofluorescence images of vinculin at the basal plane of cells on TGT-modified hydrogels. Cells were fixed in 4% formaldehyde in PBS, permeabilized with 0.1% Triton X-100, and washed in PBS. Cells were blocked with blocking buffer (1w/v% BSA in PBS) for 1 hour at 37°C. Next, cells were incubated with anti-vinculin mouse monoclonal primary antibody at 1:150 dilution, in blocking buffer (Sigma Aldrich Clone V9131) for 45 minutes at room temperature. Cells were then washed with PBS, and incubated with secondary antibody 1:500 dilution in blocking buffer (AlexaFluor 647 anti-mouse (goat IgG); Invitrogen A21236).

The vinculin staining at the basal plane were then imaged, by laser scanning confocal microscopy (20x, model LSM 710; Carl Zeiss MicroImaging). The number of vinculin positive cells and the vinculin intensity were analysed from DIC and vinculin channel images, at a magnification of 20x, by using ImageJ (<http://rsb.info.nih.gov/ij/>). The region of interest (ROI) was selected by outlining cell boundary, using the DIC images. The intensity of vinculin staining was measured from the corresponding image in the vinculin (cyan) channel. The intensity threshold in the selected ROI was set at an average pixel intensity of 10 units, due to background variation. ROIs which exhibited an average pixel intensity of less than 10 units were counted as a zero event, and cells with intensities >10units were considered vinculin positive, regardless of the relative intensity. From these data, we determined the fraction of vinculin positive cells on the different substrates (Figure S6c)

Endocytosis inhibition with MBCD

To determine whether B16F1 cells on the soft gels tore off and internalized the 12pN TGTs, we treated cells with the inhibitor Methyl- β -cyclodextrin (MBCD, Sigma Aldrich C4555). Cells were grown to confluence in DMEM with 10% FBS. At 4 hour prior to seeding the cells on the hydrogels, the confluent cells in the flask were treated with 10 mM MBCD. After 4 hour, the cells were detached with 3mM EDTA, and resuspended in 10 mM MBCD dissolved in DMEM with 0.5% FBS. The treated cells were incubated with the gels (12pN TGTs on 12kPa gels) for 30 minutes at 37 °C in a 5% CO₂ atmosphere. In order to visualize individual cells, the cell seeding density was reduced to 0.5×10^6 cells/mL, of which 30 μ l were incubated per gel,. After 30 minutes, the cells were washed with PBS and imaged. Hydrogels

were fabricated as mentioned above. In controls, we seeded untreated cells (no MBCD) on 12kPa hydrogels with 12pN TGTs. Analysis was performed using Image J software (<http://rsb.info.nih.gov/ij/>), in which the Cy3 intensity beneath cells was compared with areas without cells, for both the treated and the untreated population.

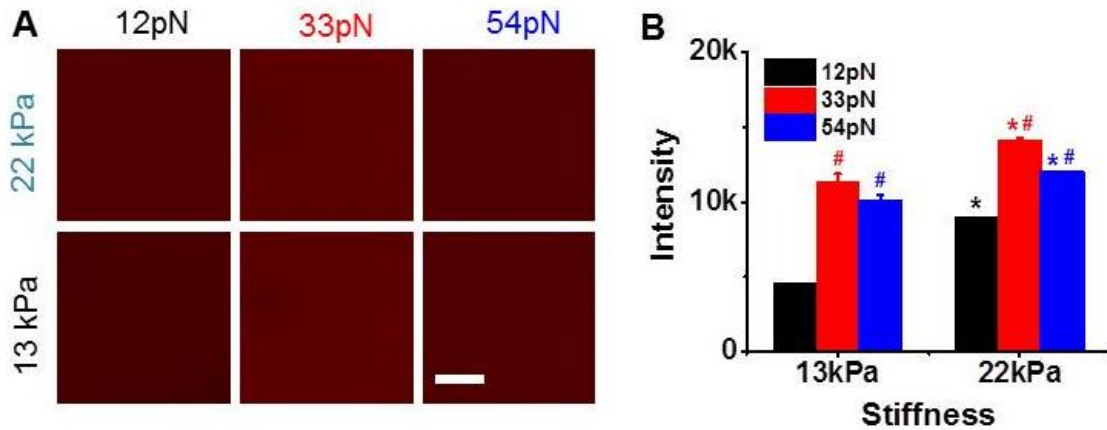


Figure S1. Comparison of TGT coverage on different substrates. (A) Fluorescence image of the surface of Cy3-labeled TGT constructs with different combinations of tension tolerance (12, 33, and 54 pN) and hydrogel stiffness (13 and 22 kPa) after washing. Scale bar 200 μ m. (B) Fluorescence intensity (arbitrary units) quantified the Cy3 fluorescence from the different gel/TGT substrate combinations shown in A. TGT fluorescence was assessed for all substrates, and the TGT concentration during polymerization was adjusted to account for potential differences in reactivity during PEGDA photopolymerization. * $p < 0.05$ between different stiffness groups and # $p < 0.05$ between different tether forces.

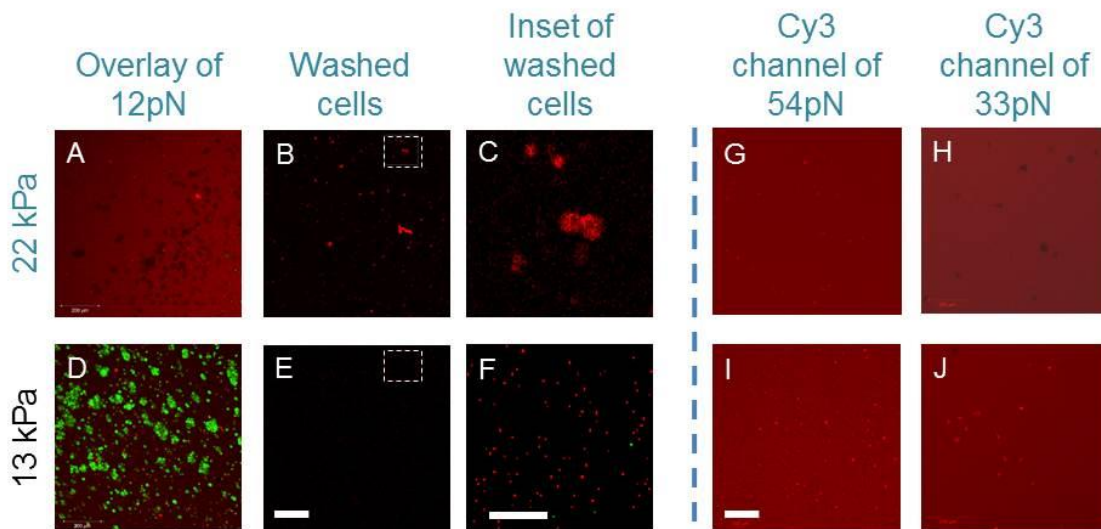


Figure S2. (A) Overlay of Calcein (green) and Cy3 (red) images of B16F1 cells on 22kPa gels modified with 12pN TGTs. (B) Cy3 image of B16F1 cells collected in the wash from the gels in A. The Cy3 cell labeling is indicative of internalized, ruptured 12pN RGD tethers. (C) Magnified image of the region of interest indicated by the white rectangle in B. (D) Overlay of Calcein and Cy3 channel images of B16F1 cells on 15kPa gels modified with 12pN TGTs. (E) Image of B16F1 cells collected from the wash of substrates in D. There were no cells with detectable levels of Cy3 uptake. (F) Magnified (63X) image of the region of interest in the white triangle in D. (G, H) Cy3 channel image of 22kPa gels with 54pN and 33pN TGTs, and seeded with B16F1 cells. A few dark footprints can be seen on the 22kPa gel modified with the 33pN tether. (I, J) Cy3 channel image of 13kPa gels modified with 54pN and 33pN TGTs and seeded with B16F1 cells (A,B,C, D,G,H) Scale bar 200 μm (E,F) Scale bar 50 μm .

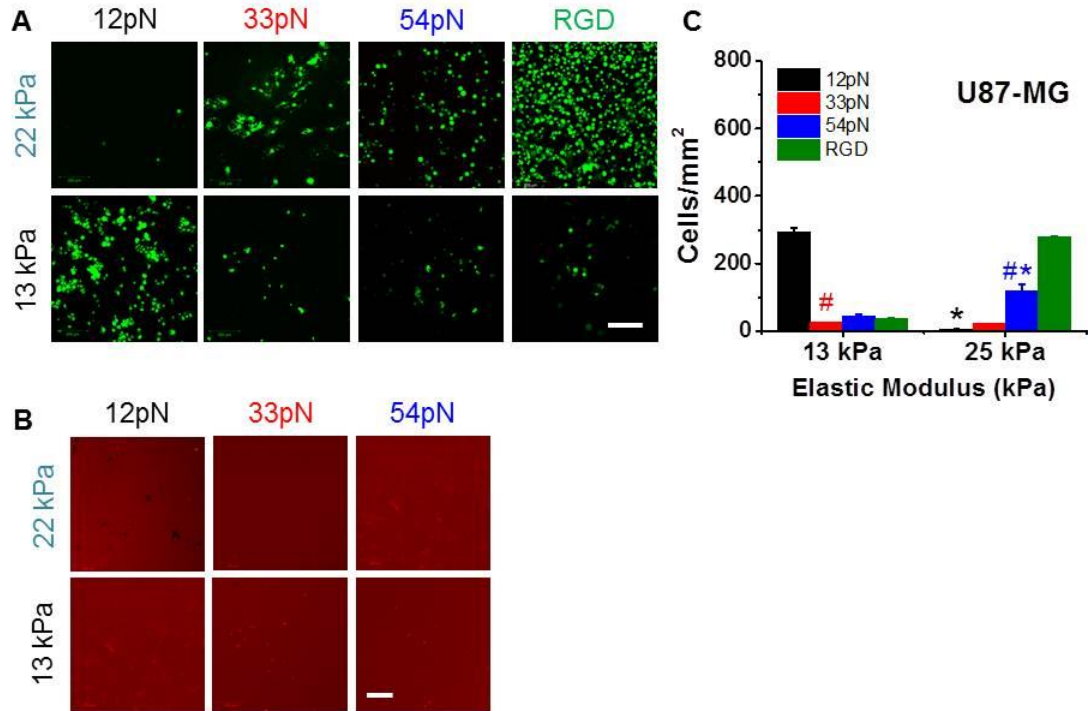


Figure S3. Confocal images of adherent glioma cells (U87-MG) on 13kPa and 22kPa substrates modified with TGTs of different tension tolerance. (A) U87-MG cells stained with Calcein A (Live/Dead assay) on the different substrates. Scale bar 200 μm . (B) Cy3 images of the indicated substrates. Scale bar 200 μm . (C) Cells/ mm^2 as a function of the substrate elastic modulus (kPa) and tension tolerance of the TGTs. * $p<0.05$ between different stiffness groups and # $p<0.05$ between different tether tolerance (within same stiffness group).

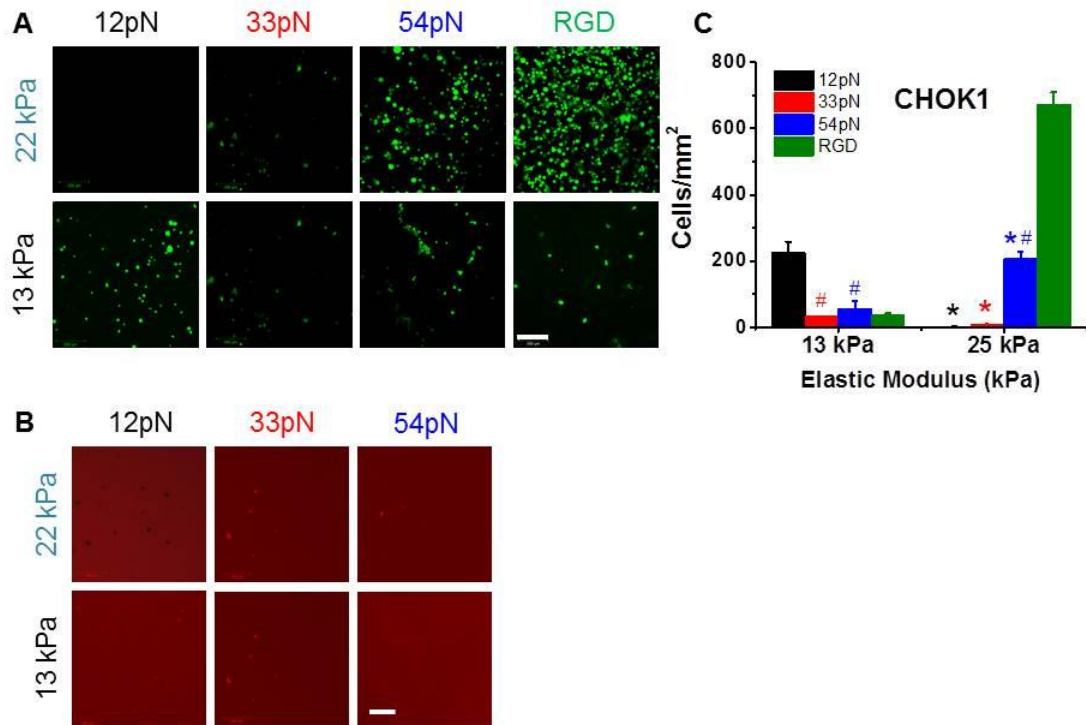


Figure S4. Confocal images of adherent CHOK1 cells on soft substrates of different stiffness and tension tolerance. (A) Calcein A stained (Live/Dead assay) CHOK1 cells on the different substrates. Scale bar 200 μm . (B) Cy3 (Red) images of the indicated substrates. Scale bar 200 μm . (C) Cells/mm² as a function of the substrate elastic modulus (kPa) and tension tolerance determined with CHOK1 cells. * $p < 0.05$ between different stiffness groups and # $p < 0.05$ between different tether forces (within the same stiffness group).

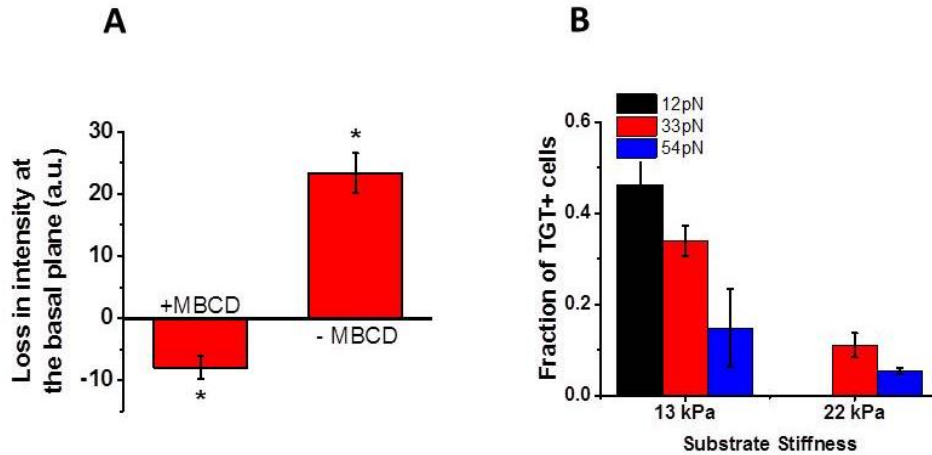


Figure S5. Tether rupture and internalization by B16F1 cells on different substrates. (A) Difference in fluorescence intensity beneath B16F1 cells on 13kPa gels with 12pN tethers \pm MBCD ($N=2$, $n_{-MBCD}=41$, $n_{+MBCD}=46$). (B) Fraction of TGT positive attached cells, which appeared red due to TGT uptake. ($n_{12pN,13kPa}=1119$, $n_{33pN,13kPa}=600$, $n_{33pN,22kPa}=132$, $n_{54pN,13kPa}=60$, $n_{54pN,22kPa}=1440$).

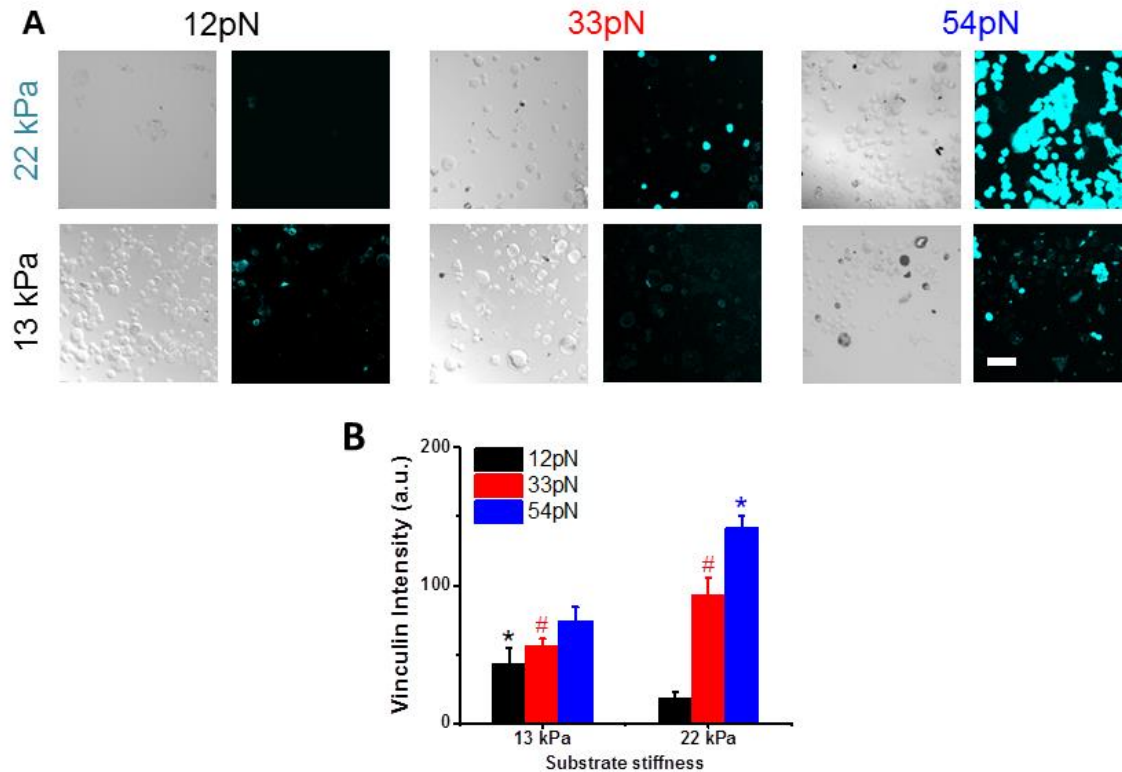


Figure S6. (A) Phase and Vinculin immunofluorescence images (20x) (cyan) of B16F1 cells on substrates of different combinations of stiffness and tension tolerance. Scale bar is 100 μ m. *Brightness and contrast of the DIC images has been adjusted. (B) Quantification of the average vinculin intensity at the basal planes of the population of cells on the different substrates ($N=2$, $n_{12pN,13kPa}=30$, $n_{33pN,13kPa}=56$, $n_{54pN,13kPa}=36$, $n_{12pN,22kPa}=8$, $n_{33pN,22kPa}=51$, $n_{54pN,22kPa}=45$). * $p<0.05$ between different stiffness groups, # $p<0.05$ between different tether forces.

	12 pN	33 pN	54 pN
22 kPa	250 ± 40	300 ± 15	390 ± 15
13 kPa	270 ± 15	310 ± 11	330 ± 15

TableS1. Cell area (μm^2) is calculated from DIC images. $n_{12\text{pN},13\text{kPa}}=50$, $n_{12\text{pN},25\text{kPa}}=24$, $n_{33\text{pN},13\text{kPa}}=50$, $n_{33\text{pN},25\text{kPa}}=50$, $n_{54\text{pN},13\text{kPa}}=50$, $n_{54\text{pN},25\text{kPa}}=50$

|

1. Franz, C. M.; Taubenberger, A.; Puech, P. H.; Muller, D. J. *Sci STKE* **2007**, 2007, (406), p15.
2. Fairbanks, B. D.; Schwartz, M. P.; Bowman, C. N.; Anseth, K. S. *Biomaterials* **2009**, 30, (35), 6702-7.
3. Chamberlain LJ, Yannas IV, Hsu HP, Strichartz G, Spector M. *Exp Neurol*. 1998 Dec;154(2):315-29.